Neuron, Vol. 16, 1209–1220, June, 1996, Copyright ©1996 by Cell Press

Protein Kinase C Enhances Exocytosis from Chromaffin Cells by Increasing the Size of the Readily Releasable Pool of Secretory Granules

Kevin D. Gillis, Rotraut Mößner, and Erwin Neher
Department of Membrane Biophysics
Max Planck Institute for Biophysical Chemistry
Am Fassberg
D-37077 Göttingen
Federal Republic of Germany

Summary

We have used membrane capacitance measurements to assay Ca^{2+}-triggered exocytosis in single bovine adrenal chromaffin cells. Brief application of phorbol ester (PMA) enhances depolarization-evoked exocytosis severalfold while actually decreasing the Ca^{2+} current. Ca^{2+} metabolism is unchanged. Three different protocols were used to show that PMA increases the size of the readily releasable pool of secretory granules. PMA treatment leads to a large increase in amplitude, but little change in the time course of the exocytic burst that results from rapid elevation of $[Ca^{2+}]_i$ upon photolysis of DM-Nitrophen. Thus, PKC appears to affect a late step in secretion but not the Ca^{2+} sensitivity of the final step.

Introduction

The activation of protein kinases by extracellular and intracellular signals often results in a profound enhancement of secretion from both neurons and neuroendocrine cells. At least in certain synapses, long-term potentiation, the standard mammalian model for short-term learning and memory, has a presynaptic component that is mediated by protein kinases (see recent reviews by Kullmann and Siegelbaum, 1995; Nicoll and Malenka, 1995). In pancreatic B cells, the activation of protein kinases is essential to support normal insulin secretion from dispersed cells (Pipeleers, 1987; Gillis and Misler, 1993; Ämmälä et al., 1993b, 1994; Barnett et al., 1994).

While the importance of protein kinases in secretion is well established, the site of action of these molecules in late steps of the stimulus-secretion cascade is not well understood. In a number of synapses, activation of cyclic AMP–dependent protein kinase (PKA) or protein kinase C (PKC) increases the frequency of spontaneous transmitter release events (e.g., Singer and Goldberg, 1969; Llano and Gerschenfeld, 1993; Capogna et al., 1995). This enhancement does not result from changes in Ca^{2+} influx or membrane excitability, leading to the common interpretation that the number of available secretory vesicles and/or the release probability of each vesicle is increased. Distinguishing between these two possibilities has proven difficult, in part because most neuronal preparations do not allow the isolation and voltage-clamp control of individual nerve terminals.

Studies in permeabilized neuroendocrine cells allow effects mediated by ionic channels to be bypassed and the intracellular Ca^{2+} concentration to be fixed to that of the extracellular medium. In pancreatic B cells, experiments of this type demonstrate enhancement of secretion by PKA (Tamagawa et al., 1985; Jones et al., 1986) and PKC (Tamagawa et al., 1985; Jones et al., 1985). Similarly, activation of PKC has been shown to enhance catecholamine release from permeabilized chromaffin cells (e.g., Knight and Baker, 1983; Pocotte et al., 1985). Recently, permeabilized cell studies have shown that the sequence in events that lead to exocytosis can be separated into early steps that require MgATP to proceed and late MgATP-independent steps (Holz et al., 1989; Hay and Martin, 1992). Within this scheme, it has been proposed that PKC enhances secretion at a late, MgATP-independent step (Bittner and Holz, 1993; Nishizaki et al., 1992; Hay and Martin, 1992). In fact, it has been suggested that PKC may enhance the Ca^{2+} sensitivity of the final step (Knight and Baker, 1983; Bittner and Holz, 1993). The time resolution of conventional biochemical assays of secretion, however, does not allow the resolution of final steps in secretion, which occur on a millisecond time scale (Thomas et al., 1993a, 1993b; Heinemann et al., 1994; Heidelberger et al., 1994).

Electrophysiological measurement of Ca^{2+}-triggered exocytosis using membrane capacitance measurements (Gillis, 1995) provides millisecond time resolution and the opportunity to directly elicit and measure the Ca^{2+} currents that trigger secretion. Alternatively, intracellular Ca^{2+} can be uniformly elevated through photorelease from caged compounds introduced into the cell through the patch pipette. Voltage-clamp studies in pancreatic B cells (Ämmälä et al., 1994) and adrenal chromaffin cells (Vitale et al., 1995) have demonstrated that PKC enhances depolarization-evoked exocytosis with only minor effects on the Ca^{2+} current.

Here, we present a detailed analysis of the enhancement of Ca^{2+}-triggered exocytosis by PKC in bovine adrenal chromaffin cells and sort out potential changes in the size of the "readily releasable pool" (RRP) of secretory granules from changes in the final Ca^{2+}-sensitive step in secretion. PKC clearly enhances the number of fusion-competent vesicles without a major change in the Ca^{2+} sensitivity of exocytosis. In addition, the Ca^{2+} current is reduced, whereas the removal of Ca^{2+} following brief depolarizing pulses is not affected.

Results

PMA Enhances Depolarization-Induced Exocytosis while Decreasing I_{Ca}

The phorbol ester PMA (phorbol 12-myristate 13-acetate) activates PKC due to its structural similarity with the endogenous activator diacylglycerol. Figure 1 presents a sample experiment in which application of 100 nM PMA leads, within seconds, to a nearly 2-fold increase in the ΔC_m response to a depolarizing pulse. This is followed by a significant drop in the peak Ca^{2+} current (I_{Ca}) and, in many cells, an increase in the rate of current inactivation. In most cells, ΔC_m responses reached a peak several minutes after exposure to PMA and then

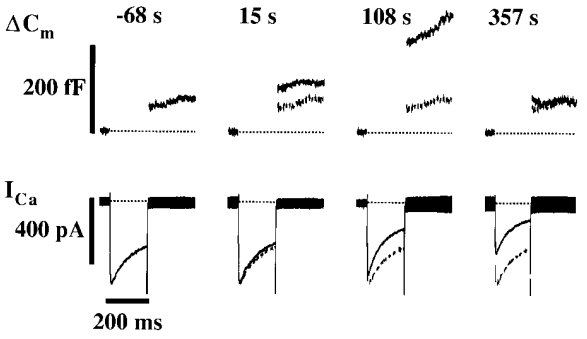

Figure 1. The Phorbol Ester PMA Leads to a Rapid Enhancement of Depolarization-Evoked Exocytosis while Actually Decreasing I_{Ca}

Sample responses from the same cell are illustrated during conventional whole-cell recording; 200 ms depolarizations to +10 mV were given every 40 s. The upper traces show the change in C_m relative to the 50 ms period before each pulse, and the lower traces display the corresponding I_{Ca}s. The indicated times are relative to application of 100 nM PMA via an application pipette. The control ΔC_m and I_{Ca} responses are overlaid with dashed lines on subsequent responses to facilitate comparison.

declined, presumably due to the continuing drop in I_{Ca} and/or a "rundown" of secretory competence. To determine whether the drop in I_{Ca} is due to a shift in the voltage dependence, I–V curves were made before and after PMA application. No shift was observed in all four cells examined (data not shown).

PMA Enhances Exocytosis through Activation of PKC. Tonic PKC Activity Does Not Contribute Greatly to Exocytosis

Since phorbol esters (and the vehicle DMSO) can have nonspecific effects, it is important to establish that the observed action of PMA is due to its activation of PKC. 4α-Phorbol 12,13-didecanoate (4α-PDD) is a phorbol ester that is often used as a control because it is ineffective in activating PKC. Figure 2A presents an experiment in which application of 50 nM 4α-PDD has no effect on depolarization-evoked exocytosis; however, a subsequent application of the same concentration of PMA enhances ΔC_m responses about 3-fold. Note that the decline in the integral of I_{Ca} (Q) occurs in PMA, but not in 4α-PDD. Similar results were seen in two other cells.

Bisindolymaleimide I (BIS) is a staurosporine derivative that is believed to be a specific inhibitor of PKC (Toullec et al., 1991). Figure 2B depicts the results of experiments in paired cells in which 100 nM PMA was applied either in the presence or absence of 500 nM BIS. Whereas BIS was able to block the enhancement of exocytosis by PMA effectively, it did not have a significant effect on exocytosis in the absence of the phorbol ester. This suggests that, under our stimulus conditions, PKC is not contributing to exocytosis in the absence of phorbol ester. Similar results with PKC inhibitors were seen in experiments in permeabilized cells (Terbush and Holz, 1990).

Ca^{2+} Buffering/Extrusion Is Unaffected by PKC

PKC has been reported to inhibit the Na^+/Ca^{2+} exchanger in chromaffin cells (Lin et al., 1994); thus, the

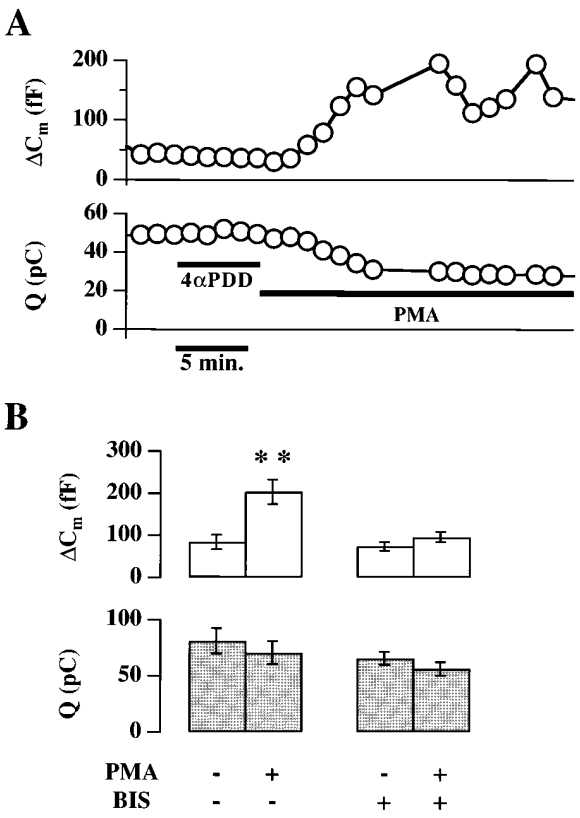

Figure 2. PMA Enhances Exocytosis through Activation of PKC

(A) 4α-PDD, a phorbol ester that does not activate PKC, has no effect on depolarization-evoked ΔC_ms or I_{Ca}s. ΔC_ms were evoked by 200 ms pulses to +10 mV every 74 s during perforated-patch recording. The bath solution contained 2 mM Ca^{2+}, rather than the usual 10 mM. 50 nM 4α-PDD, followed by 50 nM PMA were applied via bath exchange.

(B) BIS, a selective inhibitor of PKC, blocks the enhancement of exocytosis by PMA. Paired experiments were performed in the absence (8 cells) or presence (11 cells) of 500 nM BIS in both the bath and the recording pipette; 200 ms pulses to +10 mV were applied every 40 s during conventional whole-cell recording. The three responses immediately before and the three responses >1 min after acute application of 100 nM PMA were averaged for each cell. Error bars indicate SEMs. Double asterisks indicate $p < .01$ using Student's t test with each cell serving as its own control with respect to effects of PMA.

enhancement of exocytosis by PKC could be simply due to an elevation of $[Ca^{2+}]_i$. Ca^{2+} promotes exocytosis both directly in the final step(s) of secretion and indirectly by increasing the size of the RRP (von Rüden and Neher, 1993). To examine this possibility, we routinely measured cell-averaged $[Ca^{2+}]_i$ by including the Ca^{2+} indicator fura-2 in the patch pipette during experiments performed using conventional whole-cell recording. No consistent change in the $[Ca^{2+}]_i$ trace was noted upon addition of PMA. Figure 3 depicts an example, representative of 11 cells, in which the Ca^{2+} transients that result from membrane depolarization were compared before and after PMA application. The inset demonstrates, on an expanded time scale, that the peak $[Ca^{2+}]_i$, the time constant of decay, and the basal value of $[Ca^{2+}]_i$ were all unchanged by the phorbol ester.

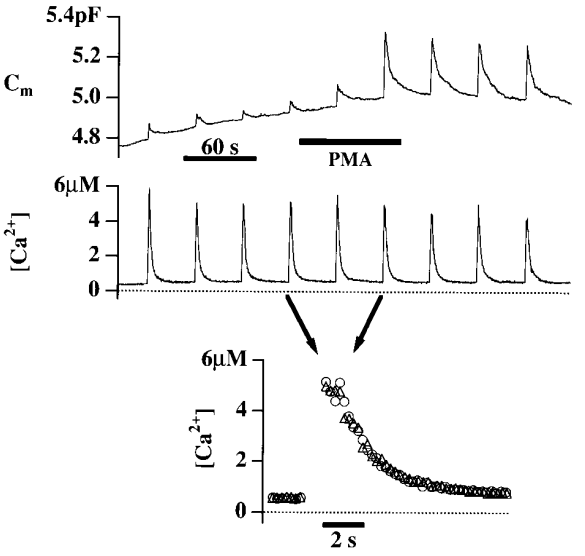

Figure 3. Application of PMA Causes no Change in Basal $[Ca^{2+}]_i$ or the Time Course of $[Ca^{2+}]_i$ in Response to a Depolarizing Pulse

Each Ca^{2+} transient results from a 200 ms depolarizing pulse to +10 mV during whole-cell recording with 100 μM fura-2 included in the recording pipette. Acute application of 100 nM PMA via an application pipette leads to a severalfold enhancement of depolarization-evoked increases in C_m that are followed by decreases presumably reflecting endocytosis. Sample Ca^{2+} transients before (circles) and after PMA application (triangles) are overlaid to illustrate that they follow the same time course.

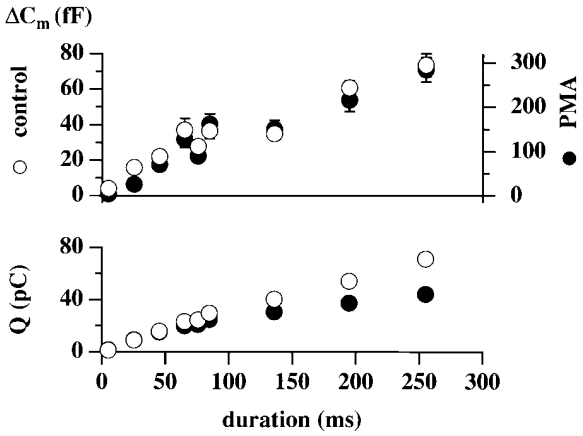

Figure 4. Increasing the Duration of Test Depolarizations Leads to a Plateau in the ΔC_m Response

Open circles denote control responses, whereas closed circles represent responses from the same 11 cells after application of 50 nM PMA. Note that a different ΔC_m scale is used for control responses versus responses elicited in the presence of PMA. Depolarizing pulses to +20 mV of various durations were applied in a scattered order every 40 s during perforated-patch recording. Several cycles were applied before and after the bath was perfused with a solution containing 50 nM PMA. Error bars indicating SEMs are depicted when larger than the symbol.

PKC Enhances the Size of the RRP of Secretory Granules

Test 1: Increasing the Duration of Test Depolarizations Leads to a Plateau in the ΔC_m Response

The concept of the RRP of vesicles originates from the observation that the rate of exocytosis declines precipitously in the presence of a constant stimulus. One method for observing the drop in secretory rate is to apply depolarizing pulses of various durations while allowing enough time between pulses to permit pool refilling (von Gersdorff and Matthews, 1994; Horrigan and Bookman, 1994). An estimate of pool size can be made if the resulting plot of ΔC_m versus pulse duration exhibits a plateau.

Figure 4 presents such a plot derived from 11 cells recorded in the "perforated patch" recording configuration (Horn and Marty, 1988) in order to allow long-term monitoring of exocytosis (Gillis et al., 1991). The open circles depict control responses, which reach a plateau value of about 34 fF (corresponding to about 14 granules) for pulses between 65 and 135 ms in duration. The responses to pulses longer than 150 ms are greater than this plateau value, suggesting the contribution of either another releasable pool or a fast refilling process.

The closed symbols depict enhanced responses from the same cells after addition of 100 nM PMA. Again, a plateau is apparent for responses between 65 and 135 ms in duration. However, the amplitude of the plateau is now approximately 130 fF.

The bottom part of the figure presents a plot of Q (the integral of I_{Ca}) versus pulse duration; the slope is the average I_{Ca}. This plot is included as a measure of I_{Ca} inactivation, since this could presumably account for the decline in the rate of exocytosis. Note that in the control responses (open circles), the plateau in the ΔC_m responses is well established by 75 ms, before any significant decline in the slope of Q versus duration. The ΔC_m responses after exposure to PMA (closed circles), however, are probably an unreliable indicator of pool size, in part because I_{Ca} inactivation is more prominent. Nevertheless, if I_{Ca} inactivation contributes to the leveling off of ΔC_m responses between 65 and 135 ms, then the actual pool size is even larger. Thus, this test still indicates that PMA enhances the size of the RRP.

Estimating the size of the RRP using the type of experiment described above, however, suffers from a couple drawbacks. First, inactivation of I_{Ca}, if significant, complicates the interpretation of the ΔC_m plateau. Second, experiments of this type are long in duration and rely on the assumptions that the RRP is refilled to the same level during the period between pulses and that I_{Ca}s are stationary. These problems prompted us to develop a "two-pulse protocol" for rapid estimation of pool size.

Test 2: ΔC_m Responses to a Pair of Depolarizing Pulses Exhibit Depression

A common technique for demonstrating the exhaustion of a putative RRP is to apply a train of depolarizing pulses and observe the decline in the ΔC_m responses with successive pulses in the train (Lim et al., 1990; Gillis and Misler, 1992; von Rüden and Neher, 1993; Ämmälä et al., 1993a; Horrigan and Bookman, 1994). A potential problem is that I_{Ca}s can also decline during the train due to inactivation. This problem can be addressed by selecting different depolarizing potentials for each of the pulses within the train so that the resulting Q values are nondecreasing (von Rüden and Neher, 1993). We

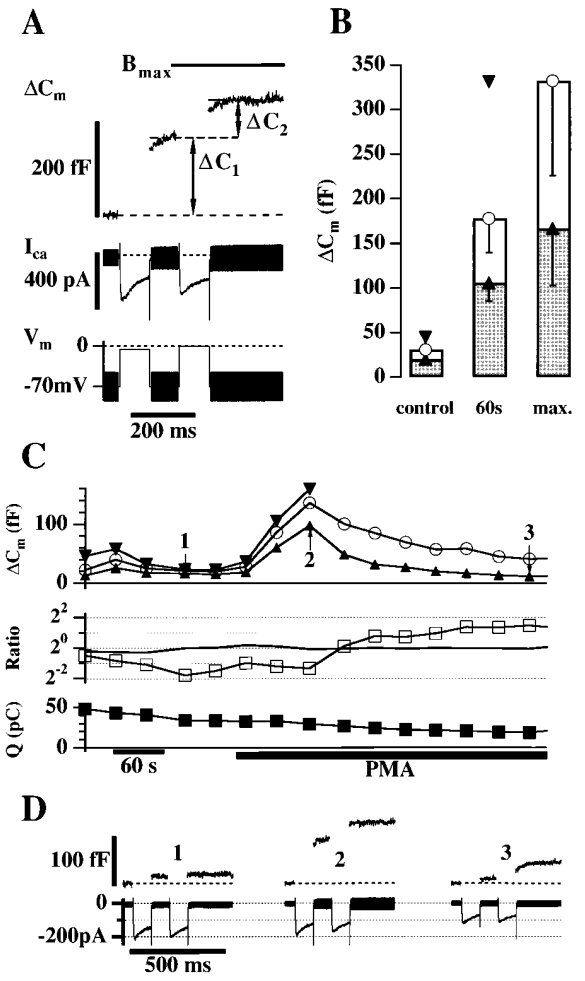

Figure 5. Use of a Dual-Pulse Protocol Indicates That PMA Increases the Size of the RRP

(A) Illustration of a dual-pulse technique for estimation of the size of the RRP. Two pulses of 100 ms duration are given 100 ms apart. The potentials of the two pulses are adjusted to give the same total amount of Ca^{2+} influx (Q). In this example, the depolarizing potentials were −5 and 0 mV and 100 nM PMA was included in the bath. The interval between pulse pairs was typically 30–60 s. ΔC_1 and ΔC_2 were measured as described in Experimental Procedures, and B_{max} was calculated according to equation 1. The pool size is then assumed to be greater than ΔC_1 but less than B_{max}.

(B) ΔC_m responses of ten cells that exhibited clear depression before application of phorbol ester. Control responses include the four pulse pairs immediately before addition of phorbol ester. The responses obtained about 1 min after adding 100 nM PMA or PDBu are depicted as are the maximal responses obtained in phorbol ester. Error bars indicate SEMs and are displayed if larger than the corresponding symbol. Upward-pointing triangles depict ΔC_1 and downward-pointing triangles indicate B_{max} from equation 1. B_{max} can not be estimated for the maximal responses because they do not show depression. Error bars for B_{max} for 1 min in phorbol ester also could not be calculated. Open circles indicate S, the sum of the two ΔC_ms. Note that ΔC_1 in PMA is larger than B_{max} in control.

(C) Sample experiment demonstrating that PMA increases the size of the RRP. The upward-pointing triangles represent ΔC_1, the open circles represent the sum of the two ΔC_ms (S), and the downward-pointing triangles are the "B_{max}" estimate from equation 1. Upward and downward triangles give quite similar estimates of pool size when clear depression of ΔC_m responses is evident. Equation 1 does not give meaningful estimates of B_{max} when ΔC_m responses exhibit facilitation (R > 1), so values are omitted in these cases. The open squares denote the ratio of the second to the first ΔC_m response (R) and the line indicates the ratio of the Q values. Note that a symmetric $\log_2$ scale is used so that the line down the middle indicates a ratio of one. Squares below the middle line depict depression, whereas squares above the middle indicate facilitation. Closed squares depict the sum of the two Q responses.

(D) Representative high-time-resolution traces are displayed for the three points indicated in (B).

have refined this technique by restricting the train to two pulses in order to simplify the analysis and choice of depolarizing potentials. We also reduced the interval between pulses to minimize the opportunity for pool refilling.

Figure 5A depicts a sample trace illustrating the protocol. ΔC_1 is the response to the first pulse and ΔC_2 is the response to the second pulse. If we define S to be the sum $\Delta C_1 + \Delta C_2$ and R to be the ratio $\Delta C_2/\Delta C_1$, then the maximum size of the RRP is given by the following (see Experimental Procedures for derivation):

$$B_{max} = S/(1 - R^2) \quad (1)$$

Equation 1 is derived with the assumption that the same fraction of the pool is released with each pulse. If residual Ca^{2+} from the first pulse leads to a greater fractional release in the second pulse (a likely possibility), or if measurable refilling of the pool occurs between pulses, then the actual initial pool size is less than B_{max}. Therefore, it is reasonable to assume that the actual pool size lies between ΔC_1 and B_{max}, where B_{max} can be calculated from equation 1 as long as depression is observed (i.e., R < 1).

Figure 5C presents the analyzed results from a typical experiment, with sample traces depicted in Figure 5D. At time 1, control responses show clear depression of a small pool (about 20 fF). At time 2, about 1 min after application of PMA, ΔC_m responses are maximal and demonstrate depression of a pool of at least 97 fF. By time 3 (about 5 min in PMA), ΔC_m responses exhibit facilitation ($\Delta C_2 > \Delta C_1$) rather than depression, presumably because I_{Ca} has dropped to a level at which the first 100 ms pulse is insufficient to exhaust the RRP. Ten cells were analyzed which exhibited clear depression (R < 0.7) in control responses. All ten cells exhibited paired-pulse facilitation after the drop in I_{Ca} that results from phorbol ester (100 nM of either PMA or phorbol 12,13-dibutyrate [PDBu]) treatment. In nine of ten cells, ΔC_1 after phorbol ester application was greater than B_{max} in control records, indicating an increase in the size of the RRP. During this set of experiments, three cells were unresponsive to phorbol esters.

Figure 5B summarizes the results obtained from these ten cells. The estimated control size of the RRP in responsive cells that exhibited depression is between 19.9 ± 1.4 fF (ΔC_1) and 44.5 ± 6.7 fF (B_{max}). About 1 min after application of phorbol ester, the RRP is between 105.7 ± 20.3 fF (a value significantly larger than control B_{max}) and 331.5 fF (the SEM can not be determined for this value because not all cells exhibit depression). The peak ΔC_1 response in phorbol ester was 167 ± 64 fF, whereas ΔC_2 was 166 ± 44 fF. Since peak responses

(which typically occur several minutes after introducing PMA) no longer show depression, B_{max} can not be estimated, and ΔC_1 probably greatly underestimates the actual pool size. Therefore, we will take the sum of the two responses (S = 333 ± 106 fF) as a crude estimate of pool size in phorbol ester. The actual size may be larger (because we did not release the entire pool with the two pulses) or smaller (because of refilling between pulses).

Test 3: The Size of the "Exocytic Burst" Increases after Application of PMA

It has recently been proposed that there is a small "immediately releasable pool" (IRP) of secretory granules located near functional Ca^{2+} channels and that fusion-competent granules located further from the sites of Ca^{2+} entry are only released with prolonged or repeated depolarizations (Horrigan and Bookman, 1994). If what we are measuring with tests 1 and 2 is such an IRP, then it is possible that a perceived increase in pool size upon activation of PKC may actually be the consequence of a sensitization of the secretory machinery to Ca^{2+}, allowing granules further from Ca^{2+} channels to be released, rather than an actual increase in the number of fusion-competent granules docked to the plasma membrane. To address this possibility and to test directly for a shift in the Ca^{2+} sensitivity of exocytosis, we elevated $[Ca^{2+}]_i$ in a step-like manner uniformly throughout the cytoplasm via photorelease of Ca^{2+} from the compound DM-Nitrophen (Kaplan and Ellis-Davies, 1988).

Flash photolysis of Ca^{2+}-loaded DM-Nitrophen led to a rapid (within about 1 ms) elevation of Ca^{2+} that decayed within several seconds. In our experiments, only the cell and the tip of the patch pipette are illuminated by the flash lamp. Therefore, the photolyzed products wash out of the cell and are replaced by unphotolyzed, Ca^{2+}-loaded DM-Nitrophen with a time constant on the order of tens of seconds (Heinemann et al., 1994). The faster decline in $[Ca^{2+}]_i$ noted in our experiments may be due to Ca^{2+} sequestration into internal organelles or extrusion across the plasma membrane because our internal solution included MgATP (see discussion in the Experimental Procedures section).

The rapid ΔC_m response to flash photolysis of DM-Nitrophen has been called the exocytic burst (Thomas et al., 1993b). In chromaffin cells, the exocytic burst typically begins with a delay of a few milliseconds and proceeds with a time course consisting of two exponential components (Heinemann et al., 1994). The rates of the exponential components are Ca^{2+} dependent, presumably reflecting the Ca^{2+} dependence of the final step(s) of exocytosis. The amplitude of the exocytic burst is commonly interpreted as the total number of fusion-competent vesicles docked to the plasma membrane at the time of the flash.

Figure 6A presents six consecutive responses to flashes in the same cell. The time between flashes was about 45 s. Application of 100 nM PMA between flashes 3 and 4 leads to a ~5-fold increase in the size of the exocytic burst (note that our internal solution contains MgATP). Since each exocytic burst presumably reflects the release of all fusion-competent granules, the vigorous responses to the fifth and sixth flashes demonstrate that this large pool can be refilled in the periods between flashes. In similar experiments, 15 out of 16 cells exhibited at least a doubling in size of the exocytic burst upon acute application of 100 nM PMA.

Figure 6B summarizes results from ten cells to which PMA is applied between the third and fourth flashes. The fifth flash gave the maximum response of 310 ± 46 fF, which compares favorably with our crude estimate from test 2 (333 ± 106 fF).

Paired experiments were also performed which compared the size of the response to the first flash in control cells versus cells incubated in PMA. The size of control responses averaged 266 ± 52 fF (n = 9), whereas cells exposed to PMA had responses of 638 ± 82 fF (n = 13).

Estimates of the size of the RRP using each of the three tests are summarized in Table 1.

The Ca^{2+} Sensitivity of Exocytosis Is Not Fundamentally Altered by PKC

If PKC increases the size of the RRP, but has no effect on the Ca^{2+} dependence of exocytosis, then exocytic bursts in control versus PMA-exposed cells should proceed with a similar time course when normalized to the total size of the response. Figure 6C depicts normalized traces averaged from three cells for flashes before (crosses) and after (line) application of PMA. Whereas PMA led to an increase in the amplitude of the exocytic burst from 36 fF to 243 fF, the time course of the response is not greatly affected.

Figure 6D presents a summary of paired experiments obtained from two batches of cells. ΔC_m responses to a first flash were fit to a sum of two exponentials, and an initial delay was determined. Open symbols denote controls, and closed symbols were obtained from cells incubated in PMA. The plot of rate constants versus $[Ca^{2+}]_i$ demonstrates a similar Ca^{2+} dependence in control versus PMA-treated cells, and no consistent shift in delays is apparent either. The solid lines are drawn between binned values taken from Heinemann et al. (1994), which are derived from control cells and are in excellent agreement with rates obtained in PMA-treated cells. In contrast with the kinetics, the amplitudes of the exponential components are quite different, with PMA-treated cells having amplitudes about 3-fold larger than control cells.

Discussion

PKC Enhances Ca^{2+}-Triggered Exocytosis

Our results confirm previous studies (e.g., Knight and Baker, 1983; Pocotte et al., 1985; Vitale et al., 1995) that show that application of a phorbol ester (PMA) leads to a severalfold increase in Ca^{2+}-triggered exocytosis from bovine adrenal chromaffin cells. We believe this effect is mediated by the activation of PKC because a control phorbol ester has no effect (Figure 2A) and a selective inhibitor of PKC largely blocks the enhancement of exocytosis by PMA (Figure 2B).

PKC does not increase depolarization-induced secretion by increasing the Ca^{2+} current (I_{Ca}); rather, a decrease in I_{Ca} was noted (Figure 1). An increase in the rate of I_{Ca} inactivation was also observed.

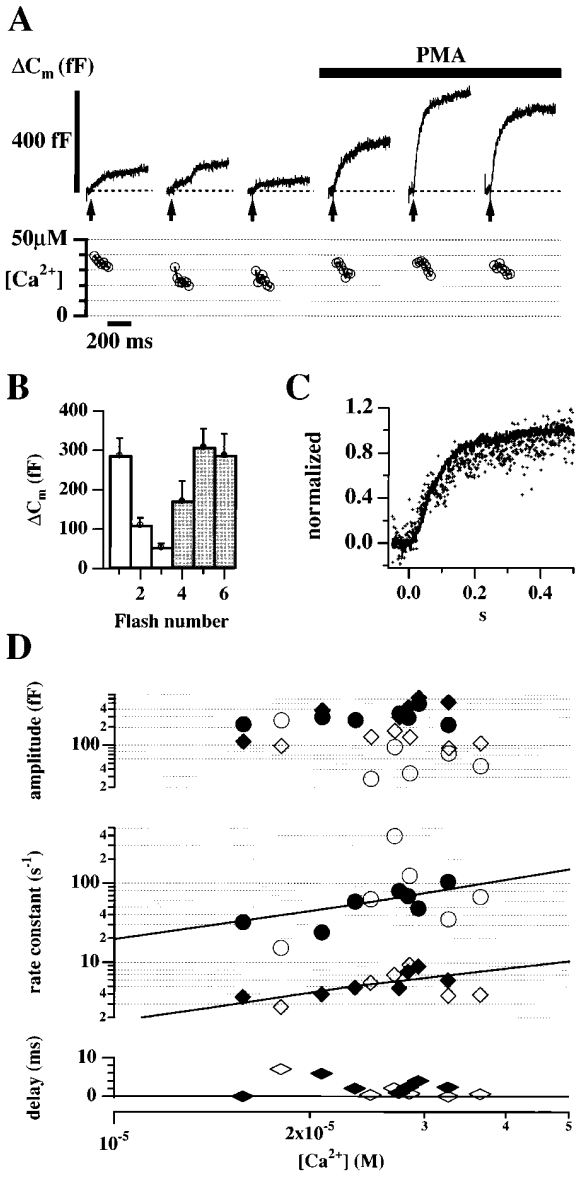

Figure 6. PMA Leads to an Increase in the Size of the Exocytic Burst That Results from Release of Caged Ca^{2+}

The Ca^{2+} sensitivity of exocytosis is not significantly shifted.

(A) Acute application of PMA leads to an increase in the exocytic burst. $[Ca^{2+}]_i$ was elevated approximately every 45 s upon flash photolysis of caged Ca^{2+} and then declined upon reequilibration with the pipette solution. The first six ΔC_m responses of an individual cell are illustrated in the top panel; 100 nM PMA was applied approximately 40 s before the fourth flash via an application pipette. The lower panel shows the estimate of $[Ca^{2+}]_i$ in the first 200 ms after the flash.

(B) The responses of ten cells recorded under the same conditions as (A); 100 nM PMA was applied between the third and fourth flashes.

(C) The time course of exocytosis is similar before and after acute application of PMA. Responses to identical intensity flashes from three cells from the same preparation were averaged and normalized to the amplitude 500 ms after the flash. The crosses are the normalized response before PMA (third flash) and the solid line is the normalized response from the same cells about 2 min after adding 100 nM PMA (fifth flash). The amplitude of the responses before normalization was 36 fF (control) versus 243 fF (in PMA).

(D) Incubation with PMA leads to larger amplitude responses to the first flash, whereas the Ca^{2+}-sensitive rate constants are unaffected. Open symbols denote first flash responses of control cells and closed symbols are responses from cells incubated for 15–75 min in 50 nM PMA. ΔC_m responses were fitted to two exponentials (diamonds, slow component; circles, fast component). The lines are drawn between binned values from Heinemann et al. (1994). Delays indicate the time after the flash where the fits cross zero amplitude.

We have found that application of PMA does not lead to significant changes in Ca^{2+} metabolism (Figure 3). This demonstration is important because a slowing of Ca^{2+} removal and/or an increase in prestimulus $[Ca^{2+}]_i$ by PMA could enhance depolarization-induced exocytosis directly through an activation of the Ca^{2+}-sensitive final step of exocytosis or indirectly by increasing the size of the RRP of secretory granules (von Rüden and Neher, 1993).

PKC Enhances the Size of the RRP of Secretory Granules

We have used three different tests for estimating the size of the RRP of granules. Each test is designed to demonstrate a decline in secretory rate in the face of a nearly constant stimulus. The amount of exocytosis that occurs before a precipitous drop in secretory rate is defined as the size of the RRP.

In test 1, we applied pulses of different durations interspersed with resting periods to allow pool refilling. Ideally, a plot of ΔC_m versus pulse duration comes to a plateau indicating pool exhaustion. Our data exhibit a clear plateau only for depolarizations between 65 and 135 ms in duration (Figure 4). From this plateau, the basal pool size was estimated to be 34 fF, corresponding to about 14 granules. The responses to pulses longer than 150 ms are significantly greater than 34 fF, suggesting the contribution of either another releasable pool or a fast refilling process. A firm estimate of the RRP after PMA application was not possible using this method, but a lower limit of 130 fF (~52 granules) could be assigned.

Test 2 applies a pair of depolarizing pulses closely spaced in time. Here, pool exhaustion is demonstrated when the ΔC_m response to the second pulse is significantly smaller than the first response (Figure 5). Equation 1 provides a way of estimating the probable maximum pool size, whereas the response to the first pulse (ΔC_1) represents an estimate of the minimum pool size. This test gave an estimate of basal pool size of between 20 (ΔC_1) and 45 fF (B_{max}), which is quite consistent with the estimate from test 1. The peak value of ΔC_1 after PMA application was 167 fF, indicating a clear increase in pool size. An upper bound for the size of the RRP in PMA could not be established because responses no longer show depression. However, a crude estimate of 332 fF (~130 granules) was made for the size of the RRP. Presumably this value (which is the peak response in PMA) is larger than the estimate from test 1 because the data set depicted in Figure 4 includes many late responses after the peak response in PMA (e.g., trace 3 of Figure 5D).

Finally, with test 3, we elevated $[Ca^{2+}]_i$ uniformly throughout the cell through flash photolysis of caged Ca^{2+}. Here, the pool size is readily estimated from the

Table 1. Estimates of the Size of theRRP of Secretory Granules

Sources of Data	Control (fF)	PMA (fF)
Test 1: ΔC_m versus duration[a]	~34 (10)	>130
Test 2: Dual-pulse protocol	20[b]–45[c] (10)	1 min, 106[b]–332[c]; peak ~333[d]
Test 3: Caged Ca^{2+} [e]		
First	266 ± 52 (9)	638 ± 82 (13)
Second	112 ± 17 (10)	—
Third	55 ± 9	—
Fifth	—	310 ± 46
Vitale et al. (1995)[f]	218 ± 53 (6)	495 ± 100 (6)
Horrigan and Bookman (1994)[g]	33.9 (26)	—

[a] Average responses to pulses between 65 and 135 ms in duration.
[b] ΔC_i.
[c] B_{max}.
[d] $\Delta C_1 + \Delta C_2$.
[e] ΔC_m measured 500 ms after flash.
[f] Sum of very first two pulses applied to a cell, 40–80 ms duration.
[g] Extrapolated from exponential fit of responses to pulses < 100 ms.
Data shown as mean ± SEM. Parentheses indicate the number of cells tested. Each cell served as its own control for tests 1 and 2. Responses to the first flash (test 3) were paired experiments. Responses to second to fifth flashes are from a different set of ten cells to which PMA was added after the third flash (see Results and Figures 6A and 6B). The first flash response for these ten cells was 288 ± 44 fF.

size of the exocytic burst (Figure 6). The size of the exocytic burst that results from the first flash is more than doubled upon preincubation with PMA (266 fF to 638 fF). Experiments in which $[Ca^{2+}]_i$ was elevated multiple times demonstrated that acute application of PMA leads to a manyfold increase in the size of the exocytic burst (Figure 6B and Table 1).

The results of each of these tests agree that application of PMA leads to a dramatic increase in the size of the RRP.

Comparison of Pool Size with Other Published Studies

An apparent discrepancy exists between the small pool size estimates obtained by the first two tests of this work and much larger estimates of the size of the RRP obtained from the experiments with caged Ca^{2+} or in previous reports from this lab (e.g., Heinemann et al., 1993, 1994; von Rüden and Neher, 1993). One possible explanation for such differences is that protocols which lead to elevated $[Ca^{2+}]_i$ between pulses will enhance the size of the RRP (von Rüden and Neher, 1993). Thus, the rather mild pattern of stimulation of tests 1 and 2 may lead to smaller steady-state pool sizes. Also, estimates generated using repetitive pulses with relatively long interpulse intervals (>0.5 s, e.g., von Rüden and Neher, 1993; Vitale et al., 1995) may overestimate the pool size if significant pool refilling occurs during the period between pulses.

Variations in pool size may also result from batch to batch variability in the responsiveness of cells. A small fraction of the cells we tested had large responses to our depolarizing protocols consistent with pool sizes previously reported. For example, the control response from the set of experiments depicted in Figure 2B was 85 ± 17 fF.

It has recently been proposed that there is a small IRP of secretory granules located near functional Ca^{2+} channels and that fusion-competent granules located further from the sites of Ca^{2+} entry are only released with prolonged or repeated depolarizations (Horrigan and Bookman, 1994). Conceivably, the discrepancy between depolarization-based estimates of pool size and estimates derived from the first photolysis of caged Ca^{2+} could arise because depolarizations only release granules near Ca^{2+} channels, whereas uniform elevation of Ca^{2+} through photolysis of DM-Nitrophen releases all fusion-competent granules (Horrigan and Bookman, 1994). It is quite interesting that Horrigan and Bookman's estimate of the size of the IRP (33.9 fF) in rat chromaffin cells is quite similar to our estimates of pool size in bovine chromaffin cells from tests 1 and 2.

An alternative explanation for the large size of the first response to photorelease of caged Ca^{2+} is that an enhancement of pool size results from the "Ca^{2+}-loading transient" that occurs shortly after attaining the whole-cell configuration as Mg^{2+} washing out of the cell displaces Ca^{2+} bound to DM-Nitrophen (Neher and Zucker, 1993; Heinemann et al., 1994). It should be noted, however, that even in the absence of a loading transient, the first responses to trains of depolarizing pulses may also be much greater than subsequent responses (Seward and Nowycky, 1996). Generally, the first few responses were excluded from our analyses using the two depolarization-based protocols. Vitale et al. (1995) presented data obtained exclusively from the first train of depolarizing pulses. The values that they obtained from their depolarization-based protocol are quite comparable with the size of the exocytic burst that we measured in response to the first flash (Table 1).

Responses to subsequent releases of caged Ca^{2+} (even in the presence of MgATP) are smaller and comparable to results from depolarization-based protocols that estimate a steady-state pool size (such as our first two tests in Table 1). For example, the response to the third release of caged Ca^{2+} was 55 ± 9 fF, whereas the estimate of basal pool size from test 2 was 20–45 fF. In addition, the crude estimate of pool size in PMA from

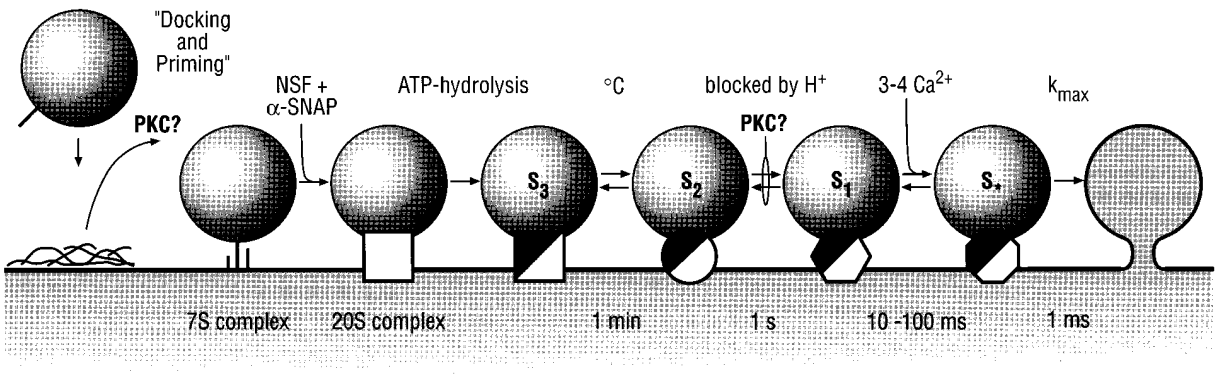

Figure 7. Kinetic Scheme for Exocytosis

Adapted from Parsons et al. (1995). PKC may be involved in early steps where disruption of a cortical actin barrier allows docking of granules (e.g., Vitale et al., 1995). Docking may also require MgATP (Parsons et al., 1995) and is followed by a step inhibited by low temperature (Bittner and Holz, 1992b; Thomas et al., 1993b), then a step inhibited by intracellular acidification (Thomas et al., 1993b). Exocytosis is triggered by the binding of 3–4 Ca^{2+} ions (Heinemann et al., 1994) and is represented as a single step for the purposes of this simplified diagram. A final step limits the maximum rate of exocytosis. PKC may act after the temperature-sensitive step (Bittner and Holz, 1993) but before the late, Ca^{2+}-sensitive step (the present work).

test 2 was 333 fF, while the response to the fifth flash (in PMA) was 310 fF.

PKC Acts at a Late, but Not Final Step in Secretion

Experiments in permeabilized neuroendocrine cells have led to the hypothesis that the sequence of events leading to exocytosis can be separated into early steps that require MgATP to proceed and late steps that are MgATP independent (Holz et al., 1989; Hay and Martin, 1992; Bittner and Holz, 1992a, 1992b). In the kinetic scheme of Bittner and Holz (1992b), PKC acts quite late in secretion, after the MgATP and temperature-dependent steps, and perhaps even at the final Ca^{2+}-sensitive step (Bittner and Holz, 1993).

A 145 kDa cytosolic protein ("p145") has been proposed to play a key role in the enhancement of secretion by PKC from mechanically permeabilized PC12 cells (Nishizaki et al., 1992). Since p145 has been assigned to a MgATP-independent "triggering" step (Hay and Martin, 1992), it is implicit that PKC also works at a late phase in secretion.

Whereas studies in permeabilized cells suggest PKC works at a late step, our results (Figure 6) indicate that PKC does not enhance the final, Ca^{2+}-sensitive trigger for secretion. The observation that PKC acts "late" in biochemical assays, yet "early" in an electrophysiological assay may simply reflect the difference in time resolution between the two techniques, and serves to bracket the site of action of PKC. Figure 7 presents a possible sequence of steps leading to exocytosis (adapted from Parsons et al., 1995). As mentioned previously, Bittner and Holz (1993) place the action of PKC after a temperature-sensitive step, which, in turn, follows an ATP-dependent reaction (Bittner and Holz, 1992b). Our placement of the effect before the final Ca^{2+}-dependent step would suggest that activation of PKC leads to an increase in the number of granules in state S_1. This could either result from an enhancement of the reaction that was shown by Thomas et al. (1993b) to be inhibited by intracellular acidification ($S_2 \rightarrow S_1$ of Figure 7) or an inhibition of the putative back-reaction ($S_1 \rightarrow S_2$).

Does PKC Act after Vesicle Docking?

Parsons et al. (1995) have shown a close correlation between the number of morphologically docked granules and the increase in C_m that can occur in the absence of MgATP. This led them to suggest that the functionally defined MgATP-independent pool is equivalent to the morphologically defined "docked" pool of secretory granules. Thus, the hypothesis that PKC acts after the ATP-dependent reaction suggests the possibility that an important effect of PKC is to speed the maturation of granules to a fully fusion-competent state after they dock with the plasma membrane.

An earlier role for PKC in enhancing the docking of secretory granules through disruption of a cortical actin "barrier" to exocytosis has also been suggested. A number of maneuvers that regulate secretion have parallel effects on cortical actin (see reviews by Burgoyne, 1991; Trifaró and Vitale, 1993). Vitale et al. (1995) have shown that application of PMA leads to a disruption of actin near the plasma membrane and an increase in the number of docked granules. It will be interesting in the future to reconcile such observations with a proposed post-MgATP role for PKC while determining which reactions are rate-limiting for secretion under different experimental protocols.

Possible Molecular Targets of PK

An understanding of how PKC modulates secretion will not be complete until the physiological substrates are identified and functionally characterized. Kinetic studies of secretion, such as this one, should then provide clues about "where" and "when" these molecules work in the secretory cascade.

Proteins believed to be involved in the regulation of cytoskeleton that are substrates for PKC include annexin I (Wang and Creutz, 1992), annexin II (Johnstone

et al., 1992), and the myristoylated alanine-rich C-kinase substrate (MARCKS; Hartwig et al., 1992).

PKC has also been proposed to interact with cytosolic proteins of unknown function that can partially restore secretion in permeabilized neuroendocrine cells. Examples include the previously mentioned p145 (Nishizaki et al., 1992) and Exo1 (Morgan and Burgoyne, 1992).

Components of the 20S SNAP–SNARE complex that have consensus site sequences for phosphorylation by PKC include SNAP-25 (Oyler et al., 1989) and α-SNAP (Whiteheart et al., 1993). Phosphorylation of Munc-18 by PKC has been reported to inhibit the association of syntaxin with Munc-18 (Fujita et al., 1996), thus freeing syntaxin to contribute to the formation of the 20S complex.

Clearly, there are many targets of PKC that are potential modulators of secretion, and so it is likely that there are multiple PKC-dependent steps in the secretory cascade. Our experimental protocols emphasize steps close to the secretory event. Therefore, the effect that we have characterized is potentially important for short-term modulation of the secretory response. In addition, the molecular target(s) involved may be participants in the intensely studied final steps of exocytosis.

Experimental Procedures

The Dual-Pulse Protocol

Derivation of Equation 1

Assume the first of the two depolarizing pulses releases the fraction α_1 of an initial pool of size B_0. The first capacitance change is then given by the following:

$$\Delta C_1 = \alpha_1 B_0$$

The second pulse releases the fraction α_2 of the remaining pool, resulting in a second capacitance change given by the following:

$$\begin{aligned}\Delta C_2 &= \alpha_2(B_0 - \Delta C_1)\\ &= \alpha_2(1 - \alpha_1)B_0\end{aligned}$$

Here, pool refilling between pulses is neglected. If we define the sum of the two responses to be S and the ratio to be R,

$$\begin{aligned}S &\triangleq \Delta C_1 + \Delta C_2\\ R &\triangleq \Delta C_2/\Delta C_1\end{aligned}$$

then algebraic manipulation yields:

$$B_0 = \frac{S}{(1 - \frac{\alpha_1}{\alpha_2} R)(1 + R)} \qquad (2)$$

If each pulse leads to the same fractional release ($\alpha_1 = \alpha_2$), then equation 1 is obtained:

$$B_{max} = S/(1 - R^2)$$

in which the notation B_{max} is used because inspection of equation 2 reveals that, if $\alpha_2 > \alpha_1$ (a likely possibility if residual Ca^{2+} from the first pulse enhances α_2), then equation 1 overestimates the initial pool size. It is also relatively straightforward to demonstrate that equation 1 is a high estimate if pool refilling occurs between the depolarizing pulses. Note that equation 1 will underestimate the initial pool size if $\alpha_1 > \alpha_2$. In this case, however, the drop in the rate of exocytosis is at least partly due to a drop in secretory efficiency and the concept of an RRP of secretory granules is not well defined.

Choosing Parameters

The actual initial pool size can be assumed to be larger than ΔC_1, but smaller than B_{max} as long as $\alpha_2 \geq \alpha_1$. To obtain a good estimate of pool size, it is desirable to make these two bracketing values as close as possible. Therefore, the objective is to minimize R (i.e., release most of the pool in the first pulse) and minimize the opportunity for pool refilling by reducing the total duration of the protocol. These two objectives are somewhat conflicting, since satisfying the first objective requires sufficiently long depolarizing pulses, whereas shorter pulses are preferable for satisfying the second objective.

Inspection of Figure 4 reveals that a pulse duration of 100 ms should, on average, be sufficient to release most of the pool with the first pulse. Large I_{Ca} also helps satisfy the first objective, so a bath solution containing 10 mM Ca^{2+} was used.

Satisfying the second objective means the interpulse interval should be as brief as possible. On the other hand, this interval should be long enough to allow the decay of the transient "gating" capacitance artifact (Horrigan and Bookman, 1994) plus the averaging of a number of C_m values to get a low noise estimate of ΔC_1. We used a total interpulse interval of 100 ms.

The depolarizing potentials used for each pulse were selected to result in the same total Ca^{2+} influx (Q). This Q value should be as large as possible to satisfy the first objective. Therefore, the potential of the second depolarizing pulse should be that which results in the peak I_{Ca} (usually +10 mV in our experiments). The potential of the first pulse was empirically selected to result in the same Q value as the second pulse. Typically, a value between −10 mV and 0 mV was used. Similar results were obtained by using potentials more depolarized than +10 mV for the first pulse (data not shown).

Cell Preparation and Solutions

Bovine adrenal chromaffin cells were prepared as previously described (Zhou and Neher, 1993) and used 1–3 days after plating. Our normal bath solution contained 140 mM NaCl, 2.8 mM KCl, 10 mM tetraethylammonium chloride (TEA-Cl), 10 mM $CaCl_2$, 1 mM $MgCl_2$, and 10 mM Na-HEPES (pH 7.2). In addition, 2 mg/ml glucose and 10 μM tetrodotoxin (TTX) were added daily.

For perforated patch recording, our internal solution contained 90 mM Cs_2SO_4, 40 mM CsCl, 8 mM NaCl, 1 mM $MgCl_2$, and 15 mM Cs-HEPES (pH 7.2). Cs^+ salts were prepared from CsOH purchased from Aldrich (Steinheim, Federal Republic of Germany). Amphotericin B was added to give a final concentration of 100–250 μg/ml (0.1%–0.25% DMSO) from a stock solution consisting of 50 mg/ml amphotericin B in DMSO. Both the stock solution and final internal solution were ultrasonicated (Sonopuls HD70, Bandeln Electronic, Berlin), stored on ice, and protected from light. The stock solution was kept frozen (−20°C) and used for about 1 week.

The internal solution used during "conventional" whole-cell recording was either the same solution used in perforated patch (see above) or a solution containing 145 mM Cs-glutamate, 8 mM NaCl, 1 mM $MgCl_2$, and 10 mM Cs-HEPES (pH 7.2). In addition, 2 mM MgATP, 0.6 mM GTP, and 0.1 mM K_5FURA (Molecular Probes, Eugene, OR) were added daily.

Stock solutions of phorbol esters were prepared at a concentration of 50–100 μM in DMSO and stored at −20°C. The final concentration of DMSO in diluted phorbol ester solutions was 0.1%. Bisindolymaleimide I (Calbiochem, Bad Soden, Federal Republic of Germany) was prepared as a 2.4 mM stock in DMSO.

All reagents are from Sigma (Deisenhofen, Federal Republic of Germany) except as otherwise noted. Experiments were performed at room temperature (21°C–30°C).

Electrophysiology

Recording pipettes were pulled from Kimax glass to a resistance of 2–4 MΩ. An EPC-9 patch clamp amplifier was used together with PULSE software (HEKA Elektronik, Lambrecht, Federal Republic of Germany). No corrections for liquid junction potentials were made for experiments using perforated-patch recording. Capacitance measurements were performed using the "software lock-in" module of PULSE. A 1 kHz, 50 mV peak-to-peak sinusoid stimulus was applied about a DC potential of −80 mV. The resulting current was processed using the Lindau–Neher technique (Lindau and Neher,

1988; Gillis, 1995) to give estimates of the equivalent circuit parameters (C_m, G_m, and G_s). The reversal potential of the measured DC current was assumed to be 0. ΔC_m values were analyzed using macros written by one of us (K. D. G.) running on Igor software (WaveMetrics, Incorporated, Lake Oswego, OR). C_m was averaged over a 50 ms predepolarization segment to give a baseline value. Pilot experiments suggested that the transient "gating" capacitance artifact (Horrigan and Bookman, 1994) was negligible 25 ms after the end of a depolarization. Therefore, C_m was averaged over the interval 25 to 75 ms after the depolarization and then the baseline C_m value was subtracted to get ΔC_m. The current during the depolarization was assumed to be predominantly carried by Ca^{2+} and was integrated to obtain Q. No correction for leak currents was made; cells with a leak greater than 200 pS were discarded. Estimates of the number of granules released are based on a value of 2.5 fF/granule (Neher and Marty, 1982). Values presented are mean ± SEM.

Caged Ca^{2+} Experiments

The hardware and calibration methods used for caged Ca^{2+} experiments were essentially identical to Heinemann et al. (1994) with the following modifications. Ca^{2+} indicator was excited (345 and 390 nm) using a monochronometer-based system (T. I. L. L. Photonics, Gräfeling, Federal Republic of Germany), and the resulting fluorescent signal was measured using a photomultiplier and sampled at 8 kHz immediately before and after the flash. Excitation was alternated between 345 and 390 nm for durations of 20 and 80 ms, respectively. The response after the flash to 345 nm excitation was fitted to a line, allowing interpolation of values to the periods of 390 nm excitation. $[Ca^{2+}]_i$ was determined from the equation (Grynkiewicz et al., 1985):

$$[Ca^{2+}]_i = K_{eff} \frac{R - R_{min}}{R_{max} - R}$$

in which K_{eff} is assigned different values before and after the flash because of bleaching of DM-Nitrophen and furaptra (Heinemann et al., 1994). Using the calibration technique of Heinemann et al. (1994), R_{min} and R_{max} were found to be 0.151 and 3.97, respectively, and were not significantly altered by the flash. K_{eff} was 2.25 mM before, and 4.354 mM after, a 300 V flash. Values for K_{eff} in the presence of neutral density filters were obtained by linear interpolation between the two values given. Postflash $[Ca^{2+}]_i$ was determined by averaging the fluorescent signal (390 nm excitation) between 30 ms and 50 ms after the flash.

The internal solution for caged Ca^{2+} experiments was designed to fulfill the following conditions: basal $[Ca^{2+}]_i < 500$ nM (the threshold for secretion), $[Ca^{2+}]_i \approx 20$ μM after 50% photolysis of DM-Nitrophen, and [MgATP] ≥ 1 mM before and after photolysis (to support phosphorylation by PKC). Furthermore, it is desirable to have DM-Nitrophen "fully loaded" with Ca^{2+} to minimize the "Ca^{2+} spike" that results from the slow binding of Ca^{2+} back onto unphotolyzed DM-Nitrophen. Since ATP is a significant Ca^{2+} buffer (K_D = 134 μM, Sillén and Martell, 1971), no other low affinity buffer was included. The internal solution contained 63 mM Cs-glutamate, 57 mM Cs-HEPES (pH 7.2), 9 mM $CaCl_2$, 3 mM MgATP, 7 mM Na_2ATP, 2 mM K_2EGTA, 1 mM furaptra, and 10 mM Na_4DM-Nitrophen (Molecular Probes, Eugene, OR). A portion of the solution was prepared with 100 μM fura-2, instead of furaptra, to allow the in vivo measurement of basal $[Ca^{2+}]$ in a set of control cells. Basal $[Ca^{2+}]$ measured this way was 200–400 nM.

Calculations were performed which take into account that DM-Nitrophen, like EDTA, binds Mg^{2+} with a reasonably high affinity (K_D = 2.5 μM, Kaplan and Ellis-Davies, 1988). Basal values were estimated to be as follows: $[Ca^{2+}]_{free}$ = 150 nM, $[Mg^{2+}]_{free}$ = 16 μM, [MgATP] = 1.28 mM. After 50% photolysis of DM-Nitrophen, equilibrium values were calculated to be $[Ca^{2+}]_{free}$ = 37 μM, $[Mg^{2+}]_{free}$ = 57 μM, and [MgATP] = 2.9 mM. Before photolysis, about 99% of furaptra is free despite the presence of Mg^{2+}. After 50% photolysis of DM-Nitrophen, Mg^{2+} represents only 3% of the divalent cations bound to furaptra, therefore this indicator gives a faithful estimate of $[Ca^{2+}]$.

Following rapid elevation by flash photolysis, $[Ca^{2+}]$ often declined with a time constant of about 1 s to levels too low to be measured by furaptra. In the experiments of Heinemann et al. (1994), the time constant of Ca^{2+} decay was on the order of tens of seconds and presumably reflected the time required for reequilibration with the unphotolyzed pipette solution. Our faster decay was probably related to the presence of MgATP in the pipette solution.

One possible source of the rapid decay in $[Ca^{2+}]$ is the complex solution chemistry that results from the competition of Mg^{2+} and Ca^{2+} for binding to DM-Nitrophen. Calculations suggest that much of the Mg^{2+} bound to DM-Nitrophen is replaced by Ca^{2+} after the flash. This exchange may take a second or longer and will lead to a "droop" in $[Ca^{2+}]$. Perhaps the presence of MgATP also supports rapid sequestration of Ca^{2+} into intracellular organelles and/or extrusion across the plasma membrane.

The decay in $[Ca^{2+}]$ following photolysis could potentially alter the kinetics of the exocytic burst and distort the estimate of the slower of the two exponential components. Photolysis of DM-Nitrophen led to a peak $[Ca^{2+}]$ between 10 and 50 μM (Figure 6D). Over this range, the slower rate constant of the exocytic burst is only approximately linearly dependent on $[Ca^{2+}]$ (Figure 6D and Heinemann et al., 1994). Simulations were performed which indicate that rate constants in excess of 2.5 s^{-1} are little affected by the drop in $[Ca^{2+}]$.

Acknowledgments

We would like to thank Dr. Ruth Heidelberger and Mirjam Haller for help setting up the caged Ca^{2+} experiments and Frauke Friedlein and Michael Pilot for cell preparation. Part of this work was conducted while K. D. G. was an Alexander von Humboldt research fellow.

The costs of publication of this article were defrayed in part by the payment of page charges. This article must therefore be hereby marked *"advertisement"* in accordance with 18 USC Section 1734 solely to indicate this fact.

Received April 3, 1996; revised May 7, 1996.

References

Ämmälä, C., Eliasson, L., Bokvist, K., Larsson, O., Ashcroft, F.M., and Rorsman, P. (1993a). Exocytosis elicited by action potentials and voltage-clamp calcium currents in individual mouse pancreatic B-cells. J. Physiol. *472*, 665–688.

Ämmälä, C., Ashcroft, F.M., and Rorsman, P. (1993b). Calcium-independent potentiation of insulin release by cyclic AMP in single β-cells. Nature *363*, 356–358.

Ämmälä, C., Eliasson, L., Bokvist, K., Berggren, P.-O., Honkanen, R.E., Sjöholm, Å., and Rorsman, P. (1994). Activation of protein kinases and inhibition of protein phosphatases play a central role in the regulation of exocytosis in mouse pancreatic β cells. Proc. Natl. Acad. Sci. USA *91*, 4343–4347.

Barnett, D.W., Pressel, D.M., Chern, H.T., Sharp, D.W., and Misler, S. (1994). cAMP-enhancing agents "permit" stimulus-secretion coupling in canine pancreatic islet β-cells. J. Membr. Biol. *138*, 113–120.

Bittner, M.A., and Holz, R.W. (1992a). Kinetic analysis of secretion from permeabilized adrenal chromaffin cells reveals distinct components. J. Biol. Chem. *267*, 16219–16225.

Bittner, M.A., and Holz, R.W. (1992b). A temperature-sensitive step in exocytosis. J. Biol. Chem. *267*, 16226–16229.

Bittner, M.A., and Holz, R.W. (1993). Protein kinase C and clostridial neurotoxins affect discrete and related steps in the secretory pathway. Cell. Mol. Neurobiol. *13*, 649–664.

Burgoyne, R.D. (1991). Control of exocytosis in adrenal chromaffin cells. Biochim. Biophys. Acta *1071*, 174–202.

Capogna, M., Gähwiller, B.H., and Thompson, S.M. (1995). Presynaptic enhancement of inhibitory synaptic transmission by protein kinases A and C in the rat hippocampus *in vitro*. J. Neurosci. *15*, 1249–1260.

Fujita, Y., Sasaki, T., Fukui, K., Kotani, H., Kimura, R., Hata, Y., Südhof, T.C., Scheller, R.H., and Takai, Y. (1996). Phosphorylation of Munc-18/n-Sec1/rbSec1 by protein kinase C. J. Biol. Chem. *271*, 7265–7268.

Gillis, K.D. (1995). Techniques for membrane capacitance measurements. In Single Channel Recording, Second Edition, B. Sakmann and E. Neher, eds. (New York, New York: Plenum Press), pp. 155–198.

Gillis, K.D., and Misler, S. (1992). Single cell assay of exocytosis from pancreatic islet B cells. Pflügers Arch. *420*, 121–123.

Gillis, K.D., and Misler, S. (1993). Enhancers of cytosolic cAMP augment depolarization-induced exocytosis from pancreatic B-cells: evidence for effects distal to Ca^{2+} entry. Pflügers Arch. *424*, 195–197.

Gillis, K.D., Pun, R.Y.K., and Misler, S. (1991). Single cell assay of exocytosis from adrenal chromaffin cells using perforated patch recording. Pflügers Arch. *418*, 611–613.

Grynkiewicz, G., Poenie, M., and Tsien, R.Y. (1985). A new generation of Ca^{2+} indicators with greatly improved fluorescence properties. J. Biol. Chem. *260*, 3440–3450.

Hartwig, J.H., Thelen, M., Rosen, A., Jammey, P.A., Nairn, A.C., and Aderem, A. (1992). MARCKS is an actin filament crosslinking protein regulated by PKC and calcium-calmodulin. Nature *356*, 618–622.

Hay, J.C., and Martin, T.F.J. (1992). Resolution of regulated secretion into sequential MgATP-dependent and calcium-dependent stages mediated by distinct cytosolic proteins. J. Cell Biol. *119*, 139–151.

Heidelberger, R., Heinemann, C., Neher, E., and Matthews, G. (1994). Calcium dependence of the rate of exocytosis in a synaptic terminal. Nature *371*, 513–515.

Heinemann, C., von Rüden, L., Chow, R.H., and Neher, E. (1993). A two-step model of secretion control in neuroendocrine cells. Pflügers Arch. *424*, 105–112.

Heinemann, C., Chow, R.H., Neher, E., and Zucker, R.S. (1994). Kinetics of the secretory response in bovine chromaffin cells following flash photolysis of caged Ca^{2+}. Biophys. J. *67*, 2546–2557.

Holz, R.W., Bittner, M.A., Peppers, S.C., Senter, R.A., and Eberhard, D.A. (1989). MgATP-independent and MgATP-dependent exocytosis. J. Biol. Chem. *264*, 5412–5419.

Horn, R., and Marty, A. (1988). Muscarinic activation of ionic currents measured by a new whole-cell recording method. J. Gen. Physiol. *92*, 145–159.

Horrigan, F.T., and Bookman, R.J. (1994). Releasable pools and the kinetics of exocytosis in adrenal chromaffin cells. Neuron *13*, 1119–1129.

Johnstone, S.A., Hubaishy, I., and Waisman, D.M. (1992). Phosphorylation of annexin II tetramer by protein kinase C inhibits aggregation of lipid vesicles by the protein. J. Biol. Chem. *267*, 25976–25981.

Jones, P.M., Stutchfield, J., and Howell, S.L. (1985). Effects of Ca^{2+} and a phorbol ester on insulin secretion from islets of Langerhans permeabilised by high-voltage discharge. FEBS Lett. *191*, 102–106.

Jones, P.M., Fyles, J.M., and Howell, S.L. (1986). Regulation of insulin secretion by cAMP in rat islets of Langerhans permeabilised by high voltage discharge. FEBS Lett. *205*, 205–209.

Kaplan, J.H., and Ellis-Davies, G.C.R. (1988). Photolabile chelators for rapid photolytic release of divalent cations. Proc. Natl. Acad. Sci. USA *85*, 6571–6575.

Knight, D.E., and Baker, P.F. (1983). The phorbol ester TPA increases the affinity of exocytosis for calcium in "leaky" adrenal medullary cells. FEBS Lett. *160*, 98–100.

Kullmann, D.M., and Siegelbaum, S.A. (1995). The site of expression of NMDA receptor-dependent LTP: new fuel for an old fire. Neuron *15*, 997–1002.

Lim, N.F., Nowycky, M.C., and Bookman, R.J. (1990). Direct measurement of exocytosis and calcium currents in single vertebrate nerve terminals. Nature *344*, 449–451.

Lin, L.F., Kao, L.-S., and Westhead, E.W. (1994). Agents that promote protein phosphorylation inhibit the activity of the Na^+/Ca^{2+} exchanger and prolong Ca^{2+} transients in bovine chromaffin cells. J. Neurochem. *63*, 1941–1947.

Lindau, M., and Neher, E. (1988). Patch-clamp techniques for time-resolved capacitance measurements in single cells. Pflügers Arch. *411*, 137–146.

Llano, I., and Gerschenfeld, H.M. (1993). β-adrenergic enhancement of inhibitory synaptic activity in rat cerebellar stellate and purkinje cells. J. Physiol. *468*, 201–224.

Morgan, A., and Burgoyne, R.D. (1992). Interaction between protein kinase C and Exo1 (14-3-3 protein) and its relevance to exocytosis in permeabilized adrenal chromaffin cells. Biochem. J. *286*, 807–811.

Neher, E., and Marty, A. (1982). Discrete changes of the cell membrane capacitance observed under conditions of enhanced secretion in bovine adrenal chromaffin cells. Proc. Natl. Acad. Sci. USA *79*, 6712–6716.

Neher, E., and Zucker, R.S. (1993). Multiple calcium-dependent processes related to secretion in bovine chromaffin cells. Neuron *10*, 21–30.

Nicoll, R.A., and Malenka, R.C. (1995). Contrasting properties of two forms of long-term potentiation in the hippocampus. Nature *377*, 115–118.

Nishizaki, T., Walent, J.H., Kowalchyk, J.A., and Martin, T.F.J. (1992). A key role for a 145-kDa cytosolic protein in the stimulation of Ca^{2+}-dependent secretion by protein kinase C. J. Biol. Chem. *267*, 23972–23981.

Oyler, G.A., Higgins, G.A., Hart, R.A., Battenberg, E., Billingsley, M., Bloom, F.E., and Wilson, M.C. (1989). The identification of a novel synaptosomal-associated protein, SNAP-25, differentially expressed by neuronal subpopulations. J. Cell Biol. *109*, 3039–3052.

Parsons, T.D., Coorssen, J.R., Horstmann, H., and Almers, W. (1995). Docked granules, the exocytic burst, and the need for ATP hydrolysis in endocrine cells. Neuron *15*, 1085–1096.

Pipeleers, D. (1987). The biosociology of pancreatic B cells. Diabetologia *30*, 277–291.

Pocotte, S.L., Frye, R.A., Senter, R.A., TerBush, D.R., Lee, S.A., and Holz, R.W. (1985). Effects of phorbol ester on catecholamine secretion and protein phosphorylation in adrenal medullary cell cultures. Proc. Natl. Acad. Sci. USA *82*, 930–934.

Seward, E.P., and Nowycky, M.C. (1996). Kinetics of stimulus-coupled secretion in dialyzed bovine chromaffin cells in response to trains of depolarizing pulses. J. Neurosci. *16*, 553–562.

Sillén, L.G., and Martell, A.E. (1971). Stability Constants of Metal-Ion Complexes (London: Alden Press).

Singer, J., and Goldberg, H.M. (1969). Evidence for a role of cyclic AMP in neuromuscular transmission. Proc. Natl. Acad. Sci. USA *64*, 134–138.

Tamagawa, T., Niki, H., and Niki, A. (1985). Insulin release independent of a rise in cytosolic free Ca^{2+} by forskolin and phorbol ester. FEBS Lett. *183*, 430–432.

Terbush, D.R., and Holz, R.W. (1990). Activation of protein kinase C is not required for exocytosis from bovine adrenal chromaffin cells. J. Biol. Chem. *265*, 21179–21184.

Thomas, P., Wong, J.G., and Almers, W. (1993a). Millisecond studies of secretion in single rat pituitary cells stimulated by flash photolysis of caged Ca^{2+}. EMBO J. *12*, 303–306.

Thomas, P., Wong, J.G., Lee, A.K., and Almers, W. (1993b). A low affinity Ca^{2+} receptor controls the final step in peptide secretion from pituitary melanotrophs. Neuron *11*, 93–104.

Toullec, D., Pianetti, P., Coste, H., Bellevergue, P., Grand-Perret, T., Ajakane, M., Baudet, V., Boissin, P., Boursier, E., Loriolle, F., Duhamel, L., Charon, D., and Kirilovsky, J. (1991). The bisindolylmaleimide GF 109203X is a potent and selective inhibitor of protein kinase C. J. Biol. Chem. *266*, 15771–15781.

Trifaró, J.-M., and Vitale, M.L. (1993). Cytoskeleton dynamics during neurotransmitter release. Trends Neurosci. *16*, 466–472.

Vitale, M.L., Seward, E.P., and Trifaró, J.-M. (1995). Chromaffin cell cortical actin network dynamics control the size of the release-ready vesicle pool and the initial rate of exocytosis. Neuron *14*, 353–363.

von Gersdorff, H., and Matthews, G. (1994). Dynamics of synaptic vesicle fusion and membrane retrieval in synaptic terminals. Nature *367*, 735–739.

von Rüden, L., and Neher, E. (1993). A Ca-dependent early step in the release of catecholamines from adrenal chromaffin cells. Science *262*, 1061–1065.

Wang, W., and Creutz, C.E. (1992). Regulation of the chromaffin granule aggregating activity of annexin I by phosphorylation. Biochemistry *31*, 9934–9939.

Whiteheart, S.W., Griff, I.C., Brunner, M., Clary, D.O., Mayer, T., Buhrow, S.A., and Rothman, J.E. (1993). SNAP family of NSF attachment proteins includes a brain-specific isoform. Nature *362*, 353–355.

Zhou, Z., and Neher, E. (1993). Mobile and immobile calcium buffers in bovine adrenal chromaffin cells. J. Physiol. *469*, 245–273.